

# Morphology and Mechanical Property of Electrospun PA 6/66 Copolymer Filament Constructed of Nanofibers

Zhi-Juan Pan\*, Hong-Bo Liu, Qian-Hua Wan

*College of Material Engineering, Soochow University, 178 East Ganjiang Road, Suzhou 215021, P. R. CHINA*

**Abstract:** A technique for spinning continuous filaments constructed of nano-scale fibers instead of non-woven obtained by general electrospinning was described in the paper. Polyamide 6/66 copolymer solution in 88% formic acid was used as the spinning material. The relationships between the fiber microstructures, filament mechanical properties and spinning parameters: spinneret tip to collector vertical distance (TD), rotation speed (RS) were investigated. Post-drawing was performed to the as-electrospun continuous filament. The research results revealed that increase of TD and RS could improve the fiber's uniaxial alignment and crystal structure, consequently the strength of the filament was enhanced. After being post-drawn, the stress and strain at break of the electrospun polyamide 6/66 copolymer filament was well improved.

**Keywords:** electrospinning, polyamide 6/66 copolymer, nanofiber filament, mechanical property morphology

## 1. Instruction

Electrospinning is a simple and inexpensive method for fabrication of sub-micro or nano-scale fibers, which was proposed at the beginning of 20th century. Zeleny J described the principle of electrospinning in 1917 [1], and in 1934 Formals elaborated the equipment and technique to electrospin chemical fibers in the USA patent 1975704 [2]. Then, in 1969 Taylor brought forward the concepts of Taylor cone and critical voltage, and obtained the voltage values at which Taylor cones formed [3]. A great number of researchers have been focusing on the electrospinning technique since the 90th of last century, and much more than 100 polymers were spun into nano-scale fiber nonwovens.

A typical electrospinning device usually includes a metallic capillary (a stainless needle) connected to a high voltage, and a collector grounded or charged to a negative voltage. When the electric field exceeds a critical value, the electrostatic force will overcome the surface tension of the polymer solution (or melt), causing a thin jet ejection from the needle tip. As this jet travels through the air, the solvent evaporates leaving behind a polymer

fiber deposited on the collector. Generally, a porous nonwoven mat is formed by electrospinning, in which nano-scale fibers randomly orient. The nanofiber nonwovens are acceptable only for some applications such as filters, wound dressings, tissue scaffolds and sensors etc [4-6]. Meanwhile, obtaining continuously aligned nanofibers and high-volume production is very important for many areas such as fiber reinforcement and device manufacture. Several techniques have been developed to align electrospun nanofibers and some breakthroughs have been made. The primary principles to electrospin uniaxial align nanofiber bundles are changing the shape of a collector, appending an assistant electric field [7-8]. Consequently, a bigger mechanical force or electric force is loaded on fibers [9-10]. So far, a lot of methods have been achieved to obtain uniaxial fiber bundles, for example, a pair of spaced electrically charged conductive plates [4,7,9-17], rotating wheel [5,18-20], rotating disk collector [16][21-22], a tip collector [8,23], an assistant electric field [6][24], near-field electrospinning [25] and grounded collector electrode water bath [26-28].

Continuous spinnability, appropriate mechanical performances for textile process and stable

\* Corresponding author's email: zhjpan@suda.edu.cn

morphologies are very important for electrospun fiber bundles (nanofiber filaments). In this paper, we described a new spinning technique to continuously electrospin nanofiber filaments for 6~10hours. The equipment includes these elements: typical electrospinning device, active solution collector, heating-drawing set and rotating mandrel. Polyamide 6/66 copolymer pellets were used as materials. The relationships between spinning parameters and microstructures, mechanical properties of the filaments were investigated. As-electrospun PA6/66 filaments were post-drawn. The functions of drawing ratio on the crystal structures, orientations and tensile properties were also discussed.

## 2. Experimental

### 2.1 Materials

Pure polyamide 6/66 copolymer pellets (Sigma Aldrich Inc.) were dissolved in 88% formic acid, and stirred to yield a 25wt% spinning solution. Pure peregol O was mixed with deionized water, and 0.5wt% bath solution was obtained. All reagents were used without further purification.

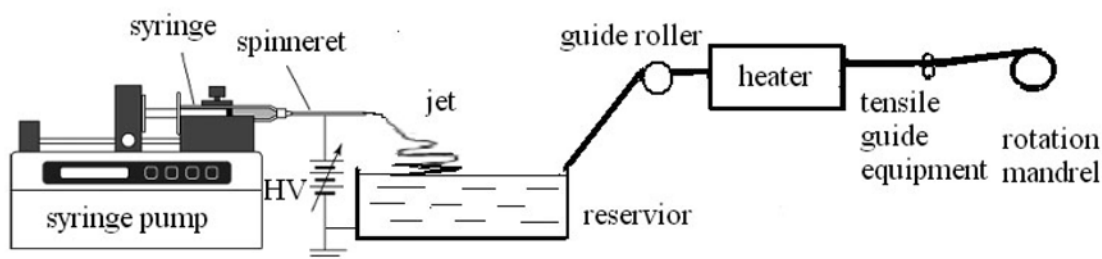


Figure 1 Schematic diagram of electrospinning device

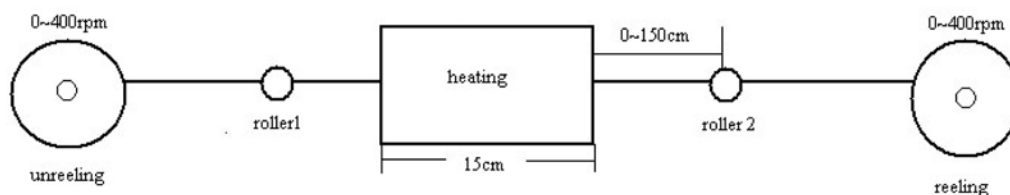


Figure 2 Sketch of post drawing of electrospun fiber bundles

### 2.2 Electrospinning nano-scale fiber filament and post drawing

As shown in Figure 1, spinning solution was drawn into a syringe with a stainless spinneret (ID 0.35mm). The spinneret was connected with a positive pole of high power supply (HV) by a wire. A circular reservoir with a diameter of 16 centimeters was full of peregol O aqueous solution. The horizontal distance from the tip of a spinneret to the left-wall of a reservoir was 2.5cm, and the vertical distance (TD) was varied. A grounded electrode was placed on the middle of the reservoir. A mandrel with diameter 11.4mm rotated on 0~400rpm, and temperature in the rotating region could be adjusted from room temperature to 400°C. The flow rate of spinning solution was controlled by a micro syringe pump (Kd scientific 100, USA).

The nano-scale copolymer PA6/66 fiber filament was formed on the following steps: Firstly, 25wt% polyamide 6/66 copolymer solution in 88% formic acid at flow rate 0.06ml/h was spun into nano-scale fibers at an electric field (voltage 14kv, TD 4~12cm), and fibers deposited on the surface of 0.5wt% bath solution. Then a bundle of continuous fibers were obtained from the reservoir, and the fiber bundle was passed through a guide roller, heater (100°C), and tensile guide equipment. Finally, continuous filament was reeled on the mandrel at 50~250 rpm. Figure 2 shows the method of post drawing electrospun fiber bundles. Both unreeling and reeling speeds are 0~400rpm. The temperature of heating region can be adjusted from room temperature to 300°C.

## 2.3 Measurements

### 2.3.1 Morphology of fiber and filament

Specimens were attached to a **copper** holder with double-sided tape, and coated with a layer of gold. Then the SEM images were observed and recorded with HITACH S-4700. The fiber diameters were calculated with HJ2000 image analysis software. 100 fibers were processed for every sample and average diameter was calculated.

A filament was cut into 10 shares with the same length and observed under an optical microscope (Leica SMLP). The filament diameters were calculated by HJ 2000 image analysis software. Every share was measured 10 times. Average diameter and the fineness unevenness were calculated from the 100 data.

### 2.3.2 Crystallinity of fiber

X'Pert Pro MPD X-ray diffraction system (CuK $\alpha$  target, acceleration voltage 40 KV, electric current 40mA,  $\lambda = 0.154$  nm) of Holand PAN alytical company was used to measure X-ray diffraction intensity curves of powdered samples, and diffraction angle  $2\theta$  ranged from  $5^\circ$  to  $45^\circ$ . The resulting plots of X-ray diffraction intensity versus  $2\theta$  were analyzed using the profile fitting program Peak Fit 4.1(AISN Software Inc.). Each peak was modeled using a Gaussian-Lorentzian peak shape. Areas of the peaks obtained from the analysis were used to estimate the degree of crystallinity.

### 2.3.3 Molecular orientation of fiber

The Raman spectrum of a single filament was obtained using a Labram 1B microscopic Raman spectrometer system (HORIBA Jobin Yvon Instrument Company, France). A filament was located under the Raman system accessorial microscope with 100X objective, and the 632.8nm He-Ne laser was focused on a  $2\mu\text{m}$  spot at the surface of the fiber to give 6mW energy. Spectral data were accumulated for 100s period at 1800 grating position.

### 2.3.4 Mechanical property of filament

Polyamide 6/66 electrospun nano-scale fiber filament with a gauge length of 10mm was deformed in tension with an Instron 3365 mechanical testing machine at crosshead speed 10mm/min, temperature of  $20\pm 2^\circ\text{C}$  and relative humidity of  $65\pm 5\%$ . Strength and elongation resolution were 0.01cN and 0.01mm respectively. All samples were balanced for 24 hours in the testing temperature and humidity, and every sample was measured 10 times.

## 3. Results and discussion

### 3.1 Effect of TD on the microstructures and tensile properties

#### 3.1.1 Effect of TD on alignment and diameter of fiber

Figure 3 is SEM images of PA6/66 fiber bundles electrospun at different TD (25wt% polyamide 6/66 solution, flow rate 0.06ml/h, RS 100rpm voltage 14kv). The fibers had no good orientation along filament axis when TD ranged 4~8cm and there were some lax loops and crossed fibers in the filaments.

When the distance between spinneret and collector is large enough, an electrospinning jet has adequate space to split into nano-scale fibers. Meanwhile, the fibers are separated by the coulomb repulsions and orient along the direction of electric field. In our research, when the vertical distance from the tip of a spinneret to the left-wall of a reservoir (TD) was increased to 10 cm, fibers aligned in uniaxial direction with few of loops (Figure 3 d). On the other hand, with the increase of TD, the area of electric field on the collector region is enlarged, resultantly, some electrospun fibers deposit on the edge of the collecting reservoir, and spinning continuity is worse.

Results listed in Table 1 revealed that the TD had no obvious effect on the average diameters and uniformities of fibers and filaments. Thus spinning distance is a sub-parameter for fiber sizes in electrospinning [29].

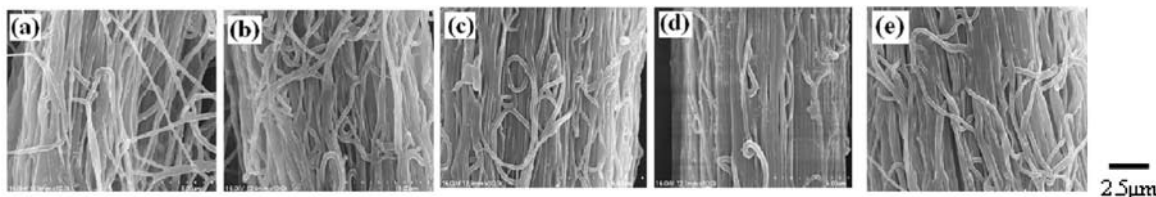


Figure 3 SEM images of PA6/66 fiber bundles electrospun at different TD (a)~(e) 4, 6, 8, 10, 12cm

Table 1 Average diameters and CV values of PA6/66 fibers and filaments electrospun at different TD (25wt% polyamide 6/66 solution, flow rate 0.06ml/h, RS 100rpm voltage 14kv)

	TD[cm] 4	6	8	10	12	
PA6/66 fiber	Average diameter[nm]	198.0	214.8	210.1	223.5	200.7
	coefficient of variation (CV) [%]	18.1	8	17.1	3	15
PA6/66 filament	Average diameter [μm]	13.7	13.1	13.1	13.7	13.7
	coefficient of variation (CV) [%]	13.1	11.3	7.0	10.4	12.3

### 3.1.2 Effect of TD on the tensile properties of filaments

Table 2 lists the crystallinities and mechanical properties of PA6/66 nanofiber filaments electrospun at different TD. As seen from the Table 2, with the increase of TD, the filament strain at break unorderly changed, but the stress at break and initial module increased. In particular, at the spinning height of 12 cm, breaking stress of the filament increased significantly. The tensile properties of PA6/66 nanofiber filaments electrospun at different TD were coincident with the alignment and degree of crystal of the fibers. The vertical distance from the tip of a spinneret to the left-wall of a reservoir (TD) is a determinant factor for the whipping and splitting of a spinning jet. A big TD supplied large space and long time for the split of an electrospinning jet, and molecular chains were induced to orient by the electric field force, so that the fiber crystal structure was improved.

## 3.2 Effect of rotating speed (RS) on the microstructures and tensile properties

### 3.2.1 Effect of RS on alignment and diameter of fiber

Considering of the function of TD on the electrospinning process and fiber alignment, PA6/66

nanofiber filaments were electrospun at TD 9cm to analyze the effect of rotating speed. The SEM photos as shown in Figure 4 suggested that the fiber alignment had been improved at fast rotating speed. Otherwise, at high rotating speed, fiber bundles endured large tension, thus fine fiber and filament was obtained (Table 3).

### 3.2.2 Effect of RS on the tensile properties of filament

Table 4, data of stress and strain at break and initial modules of PA 6/66 nanofiber filaments electrospun at different RS, indicated that rotating speed had an important effect on the electrospun nanofiber filament tensile properties. With the increase of RS, breaking strength and initial module were enhanced but strain at break, which resulted from better uniaxial alignment and improved crystallinity of fibers spun at higher speed. At higher rotating speed, a larger tension loaded on the PA6/66 nano-fibers, so that, the molecular chains formed more ordered arrangements and the crystallinities could be increased.

Table 2 Crystallinities and tensile properties of PA6/66 nanofiber filaments electrospun at different TD (25wt% polyamide 6/66 solution, flow rate 0.06ml/h, RS 100rpm voltage 14kv)

TD[cm]	4	6	8	10	12
Crystallinity [%]	36.55	40.03	41.70	44.27	54.59
Stress at break[cN/dtex]	1.21 ± 0.11	1.23 ± 0.16	1.44 ± 0.16	1.48 ± 0.23	2.22 ± 0.12
Strain at break [%]	133 ± 12.8	137 ± 5.7	109 ± 16.5	134 ± 16.3	91 ± 9.7
Initial module [cN/dtex]	6.41	6.05	7.71	7.14	11.76

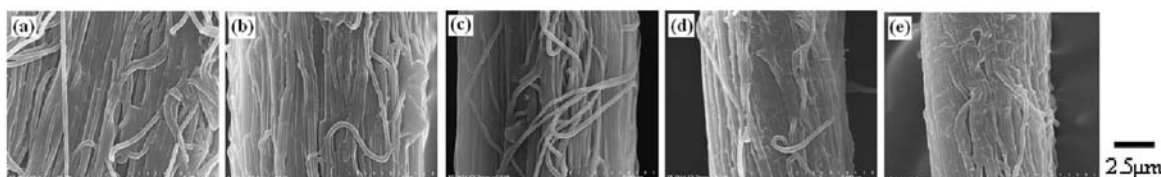


Figure 4 SEM images of PA6/66 fiber bundles electrospun at different RS. (a)~(e) 50, 100, 150, 200, 250rpm

Table 3 Average diameters and CV values of PA6/66 fibers and filaments electrospun at different RS (25wt% polyamide 6/66 solution, flow rate 0.06ml/h, TD 9cm voltage 14kv)

RS[rpm]		50	100	150	200	250
PA6/66 fiber	Average diameter [nm]	260.4	233.8	227.8	224.9	218.2
	CV [%]	16	16	16	15	18
PA6/66 filament	Average diameter [μm]	22.5	14.3	11.2	8.7	8.1
	CV [%]	16.2	10.1	8.4	9.1	10.3

Table 4 Crystallinities and tensile properties of PA6/66 nanofiber filaments electrospun at different RS (25wt% polyamide 6/66 solution, flow rate 0.06ml/h, TD 9cm voltage 14kv)

RS[cm]	50	100	150	200	250
Crystallinity [%]	42.36	42.90	43.26	44.81	44.65
Stress at break [cN/dtex]	1.24 ± 0.19	1.66 ± 0.15	1.76 ± 0.09	1.78 ± 0.17	1.84 ± 0.12
Strain at break [%]	130 ± 6.1	108 ± 13.9	104 ± 7.9	85 ± 22.7	88 ± 19.9
Initial module [cN/dtex]	6.48	7.04	9.54	7.47	14.25

Table 5 Average diameters and CV values of post drawn PA6/66 fibers and filaments

Drawing ratio		1.0	1.3	1.4	1.5	1.6	1.7
PA6/66 fiber	Average diameter [nm]	286.0	279.5	270.2	264.6	254.1	262.1
	CV [%]	23	18	18	17	22	18
PA6/66 filament	Average diameter [μm]	15.8	12.5	12.0	11.5	11.3	11.3
	CV [%]	7.5	9.1	7.3	7.2	6.4	7.3

### 3.3 Function of post drawing

PA6/66 nanofiber filament was electrospun at the following conditions: voltage 14kv, following rate 0.06ml/h, TD 9cm, peregal O aqueous solution 5wt%, rotating speed 100rpm, spinneret ID 0.35mm, 25wt% PA6/66 spinning solution. As-electrospun PA6/66 fiber bundle was post drawn 1.3, 1.4, 1.5, 1.6, and 1.7 times respectively at 100°C.

#### 3.3.1 Alignment and diameter of post drawn PA6/66 nanofiber filament

Figure 5 shows the longitudinal morphologies of post drawn PA6/66 fiber bundles and Table 5 lists diameters of these fibers and filaments. Heating post drawing improved the alignment of fibers and lessened lax loops in the filament. With the increasing of drawing ratio, fibers and filaments became thin. However, the average diameter ratios of drawn fibers / filaments to the control sample were not consistent with drawing ratios due to the transformation of fiber configuration from flabby coil / loop to stretched line in the drawing process.

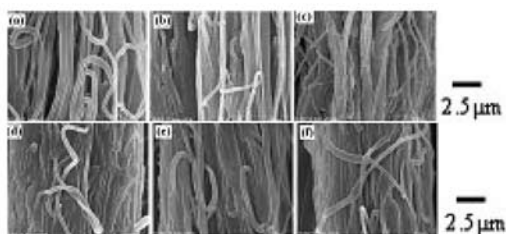


Figure 5 SEM images of post drawn PA6/66 fiber bundles (a)~(f): control, 1.3, 1.4, 1.5, 1.6, 1.7 times

#### 3.3.2 Molecular orientation and crystallinity of post drawn PA6/66 nanofiber filament

Raman spectroscopy is a powerful nondestructive technique to investigate the molecular structure of a fiber by analysis of wave numbers and intensity of spectra bands. In the Raman spectra of PA6/66 fibers shown in Figure 6, the peak bands at about 1440cm<sup>-1</sup> and 1634 cm<sup>-1</sup> are assigned to CH<sub>2</sub> bending and amide I C=O stretching[30]. The former is insensitive to the conformation, used as a standard intensity to calculate relative intensity ratios of a Raman band. Carbonyls are perpendicular to the PA6/66 macromolecule chain. If the molecules are

oriented to the fiber axis, amide I C=O stretching modes will be the strongest scatter when the direction of polarization of the laser beam is perpendicular to the fiber axis (Spectral in Figure 6). Therefore, the molecular orientation factor was calculated from the following formula:

$$f_r = \frac{x_{\perp}}{x_{\parallel}} \quad (1)$$

In which,  $f_r$  is molecular orientation factor,  $x_{\parallel} = I_{1634\parallel} / I_{1440\parallel}$ ,  $x_{\perp} = I_{1634\perp} / I_{1440\perp}$ . The  $f_r$  values (Table 6) of post drawn PA6/66 filament by electrospinning is positive correlation with drawing ratios.

It could be concluded from the crystallinity of post drawn PA6/66 fiber bundles (Table 6) and diffraction intensity curves (Figure 7) that heating stretching and oriented macromolecules would induce to form crystal.

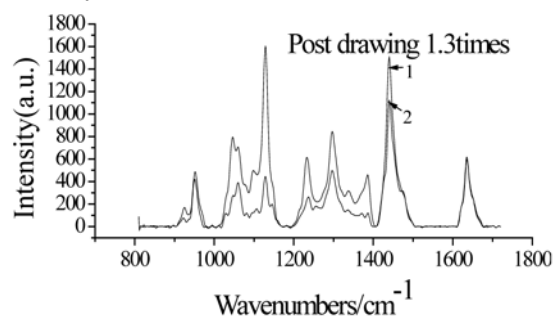


Figure 6 Raman spectra of post drawn PA6/66 fiber bundles (1- perpendicular, 2- parallel)

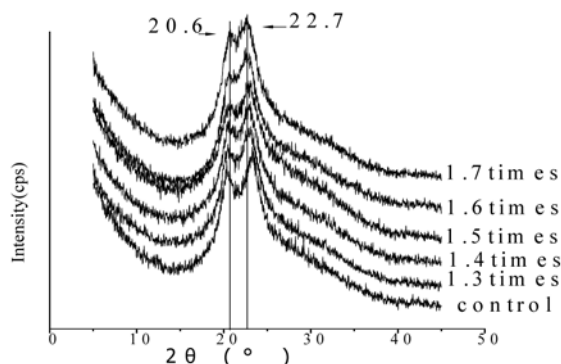


Figure 7 X-ray diffraction intensity curves of post drawn PA6/66 fiber bundles

### 3.3.3 Tensile properties of post drawn PA6/66 filament

Heating post drawing is a general method to improve the mechanical properties of as-spun chemical fibers. In our research, stretching on as-electrospun PA6/66 fiber bundles at 100°C bettered the fiber alignments,

molecular orientations and crystal structures. Consequently, the mechanical properties were improved as well. As shown in Table 6, the strength at break and initial module increased with drawing ratio, and strain at break closed to the normal level of common chemical fibers.

Table 6 Crystallinities and tensile properties of post drawn PA6/66 nanofiber filaments

Drawing ratio	1.0	1.3	1.4	1.5	1.6	1.7
$f_r$	1.01	1.31	1.58	1.70	1.77	2.03
Crystallinity[%]	42.9	47.3	48.8	46.1	45.7	49.8
Stress at break [cN/dtex]	1.66 ± 0.15	2.16 ± 0.09	2.30 ± 0.07	2.61 ± 0.07	2.77 ± 0.10	2.95 ± 0.11
Strain at break [%]	108 ± 13.9	54.5 ± 7.53	46.0 ± 3.7	33.9 ± 2.83	31.1 ± 3.44	19.1 ± 4.91
Initial module [cN/dtex]	7.04	15.2	17.6	17.8	20.4	22.7

## 4. Conclusion

A new electrospinning technique was established to spin continuous filaments constructed of nano-scale fibers. On the basis of measurement results, we concluded that: (1) Tip-to-collector vertical distance (TD) and rotation speed (RS) were the important factors for continuously fabrication of PA6/66 nanofiber filaments. Increase of TD and RS could improve the fiber's uniaxial alignment and crystal structure. Consequently the strength of the filament was enhanced. (2) After being post-drawn, the fiber alignment, molecular orientation and crystal structure of a PA6/66 nanofiber filament were obviously improved, and the stress and strain at break, initial module were optimized.

### References:

- [1] Zeleny J. Instability of electrified liquid surfaces. *Physical Review* 1917;10(1):1-6.
- [2] Formals A. Process and apparatus for preparing artificial threads. U.S. Patent No. 1975704, 1934.
- [3] Taylor GS. Sctrically driven jets. *Proc Roy London (A)* 1969;31: 353-475.
- [4] Jalili R, Morshed M, Ravandi SAH. Fundamental parameters affecting electrospinning of PAN nanofibers as uniaxially aligned fibers. *Journal of applied polymer science* 2006;101:4350-4357.
- [5] Fennessey SF, Farris RJ. Fabrication of aligned and molecularly oriented electrospun polyacrylonitrile nanofibers and the mechanical behavior of their twisted yarns. *Polymer* 2004;45:4217-4225.
- [6] Gu BK, Shin MK, Sohn KW. Direct fabrication of twisted nanofibers by electrospinning. *Appl Phys Lett* 2007;90:263-902.
- [7] Kakade MV, Givens S, Gardner K. Electric field induced orientation of polymer chains in macroscopically aligned electrospun polymer nanofibers. *J Am Chem Soc* 2007;129:2777-2782.
- [8] Rafique J, Yu J, Yu JL. Electrospinning highly aligned long polymer nanofibers on large scale by using a tip collector. *Appl Phys Lett* 2007;91:63-126.

- [9] Katta P, Alessandro M, Ramsier RD, Chase GG. Continuous electrospinning of aligned polymer nanofibers onto a wire drum collector. *Nano letters* 2004;4:2215-2218.
- [10] Li D, Wang Y L, Xia YN. Electrospinning of polymeric and ceramic nanofibers as uniaxially aligned arrays. *Nano letters* 2003;3:1167-1171.
- [11] Li D, Wang YL, Xia YN. Electrospinning nanofibers as uniaxially aligned arrays and layer-by-layer stacked films. *Adv Mater* 2004;4:361-366.
- [12] Dalton PD, Klee D, Moller M. Electrospinning with dual collection rings. *Polymer* 2005;46:611-614.
- [13] Shin MK, Kim SI, Kim SJ. Controlled assembly of polymer nanofibers: From helical springs to fully extended. *Appl Physics Lett* 2006;88:223-109.
- [14] Gao J, Yu A, Itkis ME. Large-scale fabrication of aligned single-walled carbon nanotube array and hierarchical single-walled carbon nanotube assembly. *J Am Chem Soc* 2004;26:16698-16699.
- [15] Li D, Herricks T, Xia YN. Magnetic nanofibers of nickel ferrite prepared by electrospinning. *Appl Phys Lett* 2003;83:4586-4588.
- [16] Dersch R, Liu T, Schaper AK. Electrospun nanofibers: Internal structure and intrinsic orientation. *J Polym Sci Pol Chem* 2003;41:545-553.
- [17] Tan EPS, Ng SY, Lim CT. Tensile testing of a single ultrafine polymeric fiber. *Biomaterials* 2005;26:1453-1456.
- [18] Doshi J, Reneker DH. Electrospinning process and applications of electrospun fibers. *J Electrostat* 1995;35:151-160.
- [19] Mina BM, Leea G, Kim SH. Electrospinning of silk fibroin nanofibers and its effect on the adhesion and spreading of normal human keratinocytes and fibroblasts in vitro. *Biomaterials* 2004;25:1289-1297.
- [20] Khil MS, Cha DI, Kim HY. Electrospun nanofibrous polyurethane membrane as wound dressing. *Appl Biomater* 2003;67B:675-679.
- [21] Zussman E, Theron A, Yarin AL. Formation of nanofiber crossbars in electrospinning. *Appl Phys Lett* 2003;82:973-975.
- [22] Xu CY, Inai R, Kotaki M, Ramakrishna S. Aligned biodegradable nanofibrous structure: A potential scaffold for blood vessel engineering. *Biomaterials* 2004;25:877-886.
- [23] Sundaray B, Subramanian V, Natarajan TS, Xiang RZ, Chang CC, Fann WS. Electrospinning of continuous aligned polymer fibers. *Appl Physics Lett* 2004;84:1222-1224.
- [24] Deitzel JM, Kleinmeyer JD, Hirvonen JK, Tan NCB. Controlled deposition of electrospun poly(ethylene oxide) fibers. *Polymer* 2001;42:8163-8173.
- [25] Sun DH, Chang C, Li S, Lin L. Near-field electrospinning. *Nano Lett* 2006;6: 839-842.
- [26] Khil MS, Bhattarai SR, Kim HY, Kim SZ, Lee KH. Novel fabricated matrix via electrospinning for tissue engineering. *J Biomed Mater Res B* 2005;72:117-124.
- [27] Smita E, Buttnerb U, Sanderson RD. Continuous yarns from electrospun fibers. *Polymer* 2005;46:2419-2423.
- [28] Teo WE, Gopal R, Ramaseshan R, Fujihara K, Ramakrishna S. A dynamic liquid support system for continuous electrospun yarn fabrication. *Polymer* 2007;48:3400-3405.
- [29] Tan SH, Inai R, Kotaki M, Ramakrishna S. Systematic parameter study for ultra-fine fiber fabrication via electrospinning process. *Polymer* 2005;46:6128-6134.
- [30] Song K, Rabolt JF. Polarized Raman measurements of uniaxially oriented poly ( $\epsilon$ -caprolactam). *Macromolecules* 2001;34:1650-1654.